RESEARCH PAPER

Limited genetic parallels underlie convergent evolution of quantitative pattern variation in mimetic butterflies

Hannah E. Bainbridge[1] | Melanie N. Brien[1] 🆔 | Carlos Morochz[2] | Patricio A. Salazar[1] | Pasi Rastas[3] | Nicola J. Nadeau[1] 🆔

[1]Department of Animal and Plant Sciences, The University of Sheffield, Sheffield, UK

[2]Biology & Research Department, Mashpi Lodge, Mashpi, Ecuador

[3]Institute of Biotechnology, University of Helsinki, Helsinki, Finland

Correspondence
Melanie N. Brien and Nicola J. Nadeau, Department of Animal and Plant Sciences, The University of Sheffield, Alfred Denny Building, Western Bank, Sheffield, S10 2TN, UK.
Emails: mnbrien1@gmail.com (M. N. B); n.nadeau@sheffield.ac.uk (N. J. N)

Funding information
Natural Environment Research Council, Grant/Award Number: NE/K008498/1 and NE/L002450/1

Abstract

Mimetic systems allow us to address the question of whether the same genes control similar phenotypes in different species. Although widespread parallels have been found for major effect loci, much less is known about genes that control quantitative trait variation. In this study, we identify and compare the loci that control subtle changes in the size and shape of forewing pattern elements in two *Heliconius* butterfly co-mimics. We use quantitative trait locus (QTL) analysis with a multivariate phenotyping approach to map the variation in red pattern elements across the whole forewing surface of *Heliconius erato* and *Heliconius melpomene*. These results are compared with a QTL analysis of univariate trait changes, and show that our resolution for identifying small effect loci is somewhat improved with the multivariate approach, but also that different loci are detected with these different approaches. QTL likely corresponding to the known patterning gene *optix* were found in both species but otherwise, a remarkably low level of genetic parallelism was found. This lack of similarity indicates that the genetic basis of convergent traits may not be as predictable as assumed from studies that focus solely on Mendelian traits.

KEYWORDS

adaptation, genetic architecture, *Heliconius*, Müllerian mimicry, QTL

1 | INTRODUCTION

Evolutionary convergence is the independent evolution of the same phenotype in response to the same ecological challenge (Stern, 2013). Convergent systems allow us to ask whether similar selection pressures result in similar genetic changes (Hoekstra & Nachman, 2003). Homologous loci (i.e., the same genes) can be repeatedly used by unrelated species to produce identical phenotypes

(Joron et al., 2006; Stern, 2013; Wood et al., 2005). Finding strong parallels at the genetic level suggests that there are genetic, developmental or evolutionary factors, which make certain genes more likely targets of natural selection. Nevertheless, there are also some clear cases where convergence results from different genes (Hoekstra & Nachman, 2003; Ng et al., 2008). For example, Roelants et al. (2010) report a striking example of convergence between two frog lineages, *Xenopus* and *Litoria*, which independently evolved the

same toxic skin secretions via different precursor genes (*cholecys-tokinin* and *gastrin*, respectively). Although convergent evolution refers to similar traits independently evolving in distantly related species, the term "parallel evolution" has been used to refer to the independent evolution of traits from a similar ancestral condition, or in closely related species, but at the phenotypic level, this line is clearly blurred (Arendt & Reznick, 2008). Alternatively, the term "parallel genetic evolution" can be used specifically for similar traits evolving through similar genetic pathways (Stern, 2013), and it is in this sense that we use the term. The extent to which phenotypic convergence reflects similar or divergent genetic mechanisms is still being debated.

Theoretical work suggests that adaptive evolution likely follows a "two-step" model, where species initially undergo rapid pheno-typic change, controlled by large effect loci, followed by smaller changes in order to reach a final trait optimum (Baxter et al., 2009; Nicholson, 1927; Orr, 1998; Sheppard et al., 1985). It is consider-ably easier to identify loci of large effect than those of small ef-fect that control subtle variation (Beavis, 1998; Rockman, 2011). Although high levels of genetic parallelism are often found at major effect loci between convergent species, it is likely these findings do not represent the true complexity of the genetic architecture un-derlying adaptive traits (Colosimo et al., 2005; Joron et al., 2006; Kronforst et al., 2006; Morris et al., 2019; Papa et al., 2008; Shapiro et al., 2004). Thus, if we move the focus of research away from dis-crete traits and towards the more subtle variation within quanti-tative traits, a host of small effect loci could be revealed that may differ in the extent of parallelism they exhibit (Wood et al., 2005).

Heliconius butterflies have undergone adaptive radiations into multiple colour pattern races across the Neotropics, with wide-spread phenotypic convergence between both closely and distantly related species, making the genus an ideal study system for investi-gating the level of genetic parallelism that underlies repeated evolu-tion (Hines et al., 2011; Nadeau et al., 2014; Papa et al., 2008). These toxic, warningly coloured species converge onto the same wing co-lour patterns as a mechanism to enhance predator avoidance learn-ing, a process known as Müllerian mimicry (Benson, 1972; Sheppard et al., 1985). In turn, the resultant shared local mimicry between species allows us to ask whether parallel patterns of divergence in different species are generated using parallel genetic mechanisms (Nadeau & Jiggins, 2010; Parchem et al., 2007).

To date, most of our knowledge of the genetic control of wing pattern variation in *Heliconius* comes from studies focusing on major Mendelian genes, which control specific pattern elements (Baxter et al., 2008; Naisbit et al., 2003; Papa et al., 2008). These studies have identified a set of 5 "toolkit" loci, thought to control most of the pattern variation across the genus. On chromosome 15, the gene *cortex* controls yellow and white colour pattern elements (Joron et al., 2006; Nadeau et al. 2016), whereas the transcrip-tion factor *optix* (chromosome 18) is responsible for most red and orange elements (Hines et al., 2011; Reed et al., 2011). The *WntA* gene (chromosome 10) controls various colour pattern characteris-tics by controlling the size and shape of the black pattern elements,

which in turns affects the appearance of the coloured areas (Martin et al., 2012). A further locus, *K*, switches between white and yellow colour elements, and this was recently shown to be due to a dupli-cation of the transcription factor *aristaless*, found on chromosome 1 (Westerman et al., 2018). Finally, the locus *Ro* (chromosome 13) con-trols rounding and shape of the forewing band (Nadeau et al., 2014; Sheppard et al., 1985), and this is thought to be the gene *ventral veins lacking* (Van Belleghem et al., 2017; Morris et al., 2019); and the homologue of the *Drosophila ventral veins lacking (vvl)* gene re-quired for cell proliferation and differentiation of wing veins (de Celis et al., 1995).

Heliconius has therefore been one of the taxa contributing to the paradigm that a high level of genetic parallelism exists between convergent species. However, there is limited genetic information for the more subtle variation in colour patterns, which is likely to be controlled by a larger number of small effect loci (Fisher, 1930; Wood et al., 2005). The handful of studies that have investigated quantitative pattern variation in *Heliconius* found that the toolkit loci also control this subtler variation in pattern to a greater or lesser extent (Baxter et al., 2009; Huber et al., 2015; Jones et al., 2012; Morris et al., 2019; Papa et al., 2013; Van Belleghem et al., 2017). However, no studies have directly investigated the extent of parallelism in the loci and ar-chitecture of quantitative trait variation in co-mimetic races.

In this study, we analyse quantitative variation in red forewing (FW) pattern between closely related subspecies of the co-mimics *Heliconius melpomene* and *Heliconius erato* from Panama and western Ecuador. Variation in the size and shape of the red band in these subspecies (or races) also segregates across a hybrid zone between Colombia and Ecuador and likely represents a natural evolutionary transition, allowing us to identify the loci underlying this parallel adaptive change. By analysing the pattern variation between races in a quantitative framework, we can objectively capture subtleties in pattern variation across the entire wing surface, allowing us to consider multiple axes of trait variation at once (hereafter, multivar-iate trait analysis), rather than simple discrete trait changes (Huber et al., 2015; Jones et al., 2012). The power of mapping studies to detect causal loci has been shown to greatly increase when the mul-tivariate nature of trait changes is considered (Schmitz et al., 1998). Therefore, we use this approach to address the question of whether the same loci with the same distribution of effect sizes have been used during the convergence of these two species.

2 | MATERIALS AND METHODS

2.1 | Experimental crosses

Heliconius erato demophoon and *H. melpomene rosina* individuals from Gamboa, Panama (9.12°N, 79.67°W), were single pair-mated with *H. erato cyrbia* and *H. melpomene cythera* individuals, respectively, from Mashpi, Ecuador (0.17°N, 78.87°W), to produce F_1 hybrid offspring. Crossing F1 individuals together then generated F2 offspring, whereas one *H. erato* backcross (BC) was produced by mating an F1 male with a

H. e. cyrbia female (Figure 1). The *H. erato* broods were used in a previous analysis of iridescent colour variation (Brien et al., 2018). Within

at 2× higher concentration within the pooled library to produce a higher depth of coverage.
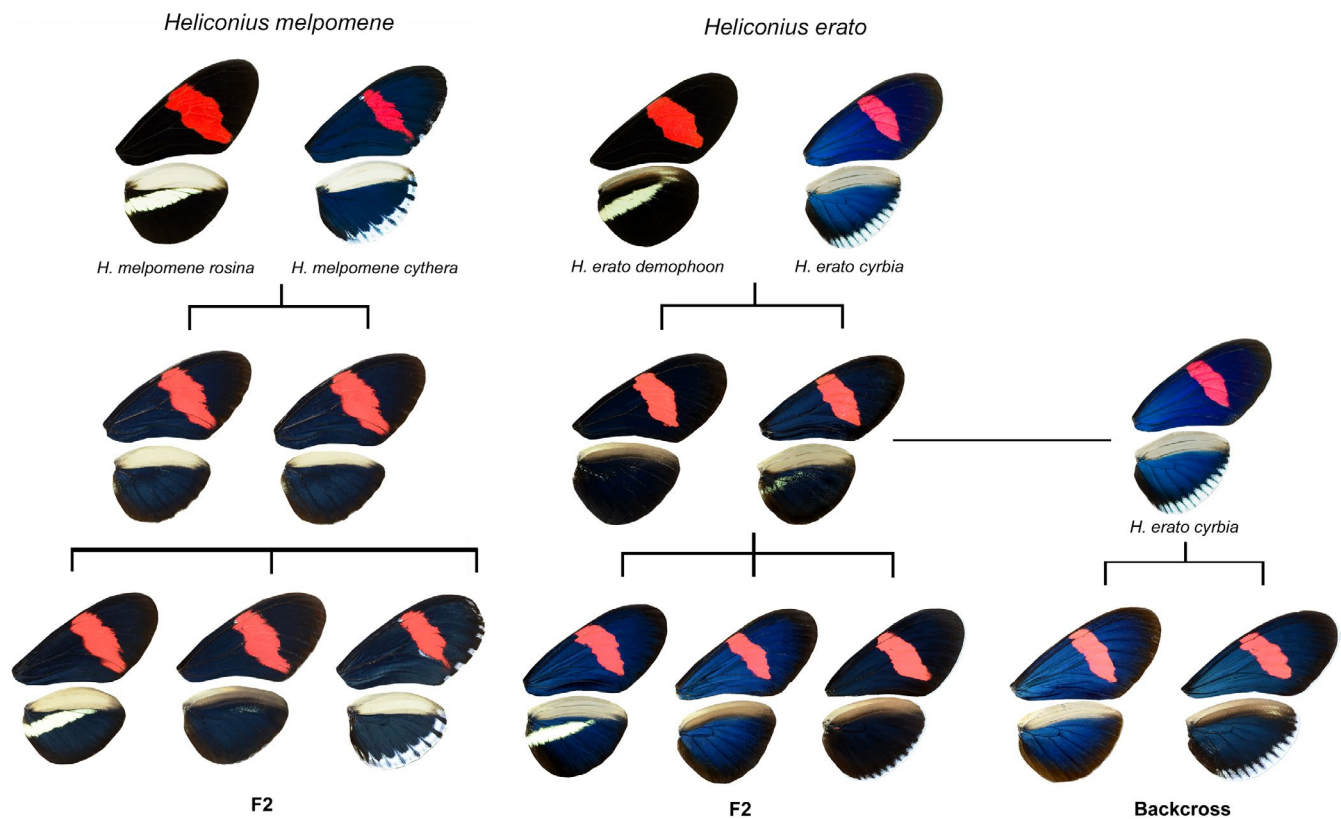

FIGURE 1 Cross-design and examples of colour pattern variation in *H. melpomene* and *H. erato*: F1, F2 and backcross (BC) generations (adapted from Brien et al., 2018)

a few hours of emergence, adult wings were removed and stored in glassine envelopes and bodies were stored in NaCl saturated 20% dimethyl sulfoxide (DMSO) 0.25 M EDTA solution to preserve the DNA. In total, three *H. melpomene* families were sequenced and used in the final analyses (two grandparents, five parents and 113 F2 offspring), along with six *H. erato* families (five grandparents, 11 parents, 99 F2 offspring and 40 backcross offspring). A further 184 *H. melpomene* and 93 *H. erato* individuals were included in the principal component analysis (PCA). Full details of all crosses are in Table S1.

2.2 | DNA extraction and sequencing

Genomic DNA was extracted using the Qiagen DNeasy Blood & Tissue Kit following the manufacturer's instructions, with an additional treatment with Qiagen RNase A to remove RNA. Approximately half of the thorax of each individual was used in the extraction. Single-digest Restriction site-associated DNA (RAD) library preparation and sequencing were carried out by the Edinburgh Genomics Facility at the University of Edinburgh. DNA was digested with the enzyme *PstI*, which has a cut site approximately every 10 kb. Libraries were sequenced on an Illumina HiSeq 2500 producing 125-bp paired-end reads. Available parents of the crosses were included

2.3 | Sequence data processing

The RADpools function in RADtools version 1.2.4 was used to demultiplex the RAD sequences, using the option to allow one mismatch per barcode (Baxter et al., 2011). Quality of all raw sequence reads were checked using FastQC (version 0.11.5; Babraham Bioinformatics). FASTQ files were mapped to the *H. erato* v1 reference genome (Van Belleghem et al., 2017) or the *H. melpomene* v2.5 reference genome (Davey et al., 2017) using bowtie2 v2.3.2 (Langmead & Salzberg, 2012). BAM files were then sorted and indexed with SAMtools (v1.3.1). PCR duplicates were removed using Picard tools MarkDuplicates (v1.102). Genotype posteriors were called with SAMtools mpileup (Li, 2011), set to a minimum mapping quality of 10 and minimum base quality of 10, using Lep-MAP data processing scripts (Rastas, 2017).

2.4 | Genetic map construction

The SNP data were constructed into linkage maps using Lep-MAP3 (Rastas, 2017). This programme is designed to work with low coverage whole genome (or reduced representation) sequencing data sets and can use pedigree information to impute and error correct SNP markers to infer chromosomal inheritance patterns and
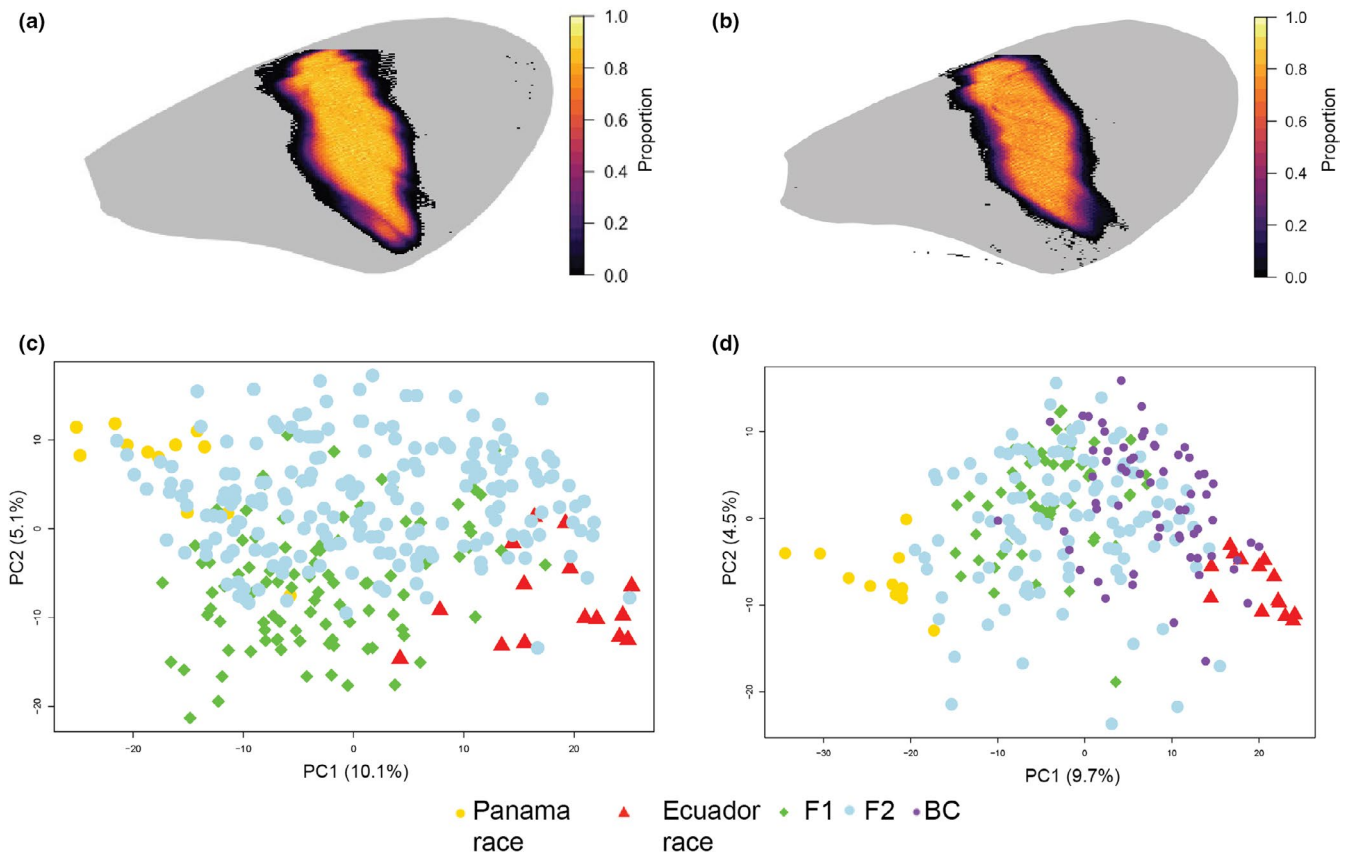
—WILEY—

FIGURE 2 Multivariate analysis of quantitative variation in red FW band shape, showing heat maps for the variation in the F2 generation of *H. melpomene* (a) and *H. erato* (b). The colour relates to the proportion of individuals that have red pigmentation at each pixel, where darker colours indicate greater variation. Principal component analyses of all individuals across the different crossing generations show how the parental variation segregates in *H. melpomene* (c) and *H. erato* (d). Note only PC1 and PC2 are shown here

recombination breakpoints. Before starting, the sex of each individual was confirmed by comparing the depth of coverage of the Z chromosome against a single autosome. Females have half the depth of coverage on the Z compared with the autosomes, as they only have one copy of the Z. Based on this, one *H. melpomene* individual was removed when the inferred sex could not be verified using the wings. The IBD module was run to verify the pedigree, and a further two individuals (one *H. erato*, one *H. melpomene*) were removed when the ancestry could not be confirmed.

We calculated and imputed the most accurate parental genotypes and sex chromosomal markers using information from related parents, grandparents and offspring, using the ParentCall2 module (with options ZLimit = 2 to also call markers on the Z chromosome and removeNonInformative = 1). Markers were then filtered to remove those with high segregation distortion (dataTolerance = 0.001). Next, markers were assigned to 21 linkage groups with the SeparateChromosomes2 module, which calculates LOD scores between pairs of markers. For *H. melpomene*, LOD limits between 10 and 25 were tested within this module, and a limit of 23 used, as this gave the correct number of linkage groups with an even distribution of markers. For *H. erato*, markers were separated into 21 linkage groups based on the chromosomal reference genome, and

then, a LOD limit of 10 was used only between markers in each of these groups, keeping the largest group per chromosome.

We added additional single markers to the existing linkage groups (with JoinSingles2all) and ordered the markers within each linkage group by maximizing the likelihood of the data (using OrderMarkers2). We assumed no recombination in females, as is standard in Lepidoptera (recombination2 set to 0) (Suomalainen et al., 1973), and male recombination was set to 0.05 (following Morris et al., 2019). The final map contained phased chromosomal marker data with imputed missing genotypes (using parameter outputPhasedData = 1). For the *H. melpomene* map, additional parameter hyperPhaser was provided to improve phasing of markers. For the *H. erato* map, the marker order was further checked against the marker order in the reference genome via parameters evaluateOrder = order.txt and improveOrder = 0, where order.txt contained the markers in the physical order from the reference.

Finally, we used LMPlot to visualize the maps and check for errors in marker order. Any erroneous markers that caused long gaps at the beginning or ends of the linkage groups were manually removed. Genotypes were phased using Lep-MAP's map2genotypes.awk script, and markers were named using the map.awk script and a list of the SNPs used to provide the scaffold name and

position. Markers that had grouped to the wrong linkage group based on genomic position were removed (<1% of the total markers). The final genetic map for *H. erato* contained 5,648 markers spread over 21 linkage groups with a total length of 1,162.4 cM (Table S2), and for *H. melpomene*, the final map had 2,163 markers spanning 1,469.9 cM (Table S3).

2.5 | Phenotypic analysis of the broods

Wings were photographed using a mounted Nikon D7000 DSLR camera with a 40 mm f/2.8 lens set to an aperture of f/10, shutter speed of 1/60 and ISO of 100, and paired Kaiser Fototechnik RB 5004 lights with daylight bulbs. All photographs also included an X-Rite Colour Checker to help standardize the colour of the images. RAW format images were standardized using the levels tool in Adobe Photoshop CS2 (Version 9.0).

Red, green and blue values for red pattern elements were selected via the *patternize* sampleRGB() function in R (R Core Team, 2018; Van Belleghem et al., 2018). These were 218, 77 and 46 for *H. erato* and 211, 1 and 30 for *H. melpomene*. *patternize* used these values to extract the presence and distribution of red pattern elements across the dorsal side of each forewing. "Offset" values were incrementally increased until coloured areas included as much of the red forewing pigmentation as possible, while minimizing the amount of background "noise" included (Hemingson et al., 2019). The final values were 0.24 for *H. erato* and 0.35 for *H. melpomene*.

To align the images, eighteen landmarks at wing vein intersections (Figure S1) were manually set, using the Fiji distribution of ImageJ (Schindelin et al., 2012). Landmark registration within the *patternize* package was used to align and extract the red pattern elements from each generation of the crosses. The variation extracted was summarized in a PCA, allowing us to examine the patterns of variation and covariation both among the red pattern element data and across the different generations (Lee et al., 2018). Additionally, *patArea()* was used to calculate the relative area of the colour pattern.

Linear measurements were also taken on the dorsal side of the forewings, to measure how far towards the distal edge of the forewing the red band extended (hereafter, "distal extension of the red FW band"). Using wing veins as fixed reference points, a measurement was taken along the lower edge of the red FW band. Three other wing measurements were also taken to standardize for wing size (Baxter et al., 2009; Figure S2). Measurements were carried out using ImageJ and repeated for both left and right wings. Final values were then calculated by taking the average of the two band measurements and dividing it by the average of all the standardizing measurements.

2.6 | Quantitative trait locus mapping analysis

Quantitative trait locus scans were carried out across the 20 autosomes using R/shapeQTL (Navarro, 2015) for multivariate

traits (principal components from the PCA) and R/qtl (Broman & Sen, 2009) for univariate traits (red band area and linear measurement). Analyses were run separately for *H. melpomene* F2, *H. erato* F2 and the *H. erato* backcross. The Z sex chromosome had to be excluded from the R/shapeQTL analysis but was included in the R/qtl analysis. Sex was included as an additive covariate in all analyses to account for possible sexual dimorphism in FW band elements (Klein & de Araújo, 2013). For analysis of F2 crosses, family was also included as a covariate.

For R/qtl analyses, the Haley–Knott (HK) algorithm was implemented to map QTL for area and FW band extension. Statistically significant LOD thresholds were calculated using 1,000 permutations (Churchill & Doerge, 1994) with *perm.Xsp = T* to get a separate threshold for the Z chromosome. The test for linkage on the sex chromosome has 3 degrees of freedom compared with 2 for the autosomes, so more permutation replicates are needed (21,832 for *H. erato* and 12,918 *H. melpomene*, compared with 1,000 permutations on autosomes) and the significance threshold is higher for the Z chromosome (Broman et al., 2006). For each QTL above the LOD threshold, 95% Bayesian credible intervals were computed using *bayesint()* to refine its boundaries. To calculate the phenotypic variance that each QTL explained, we used a multiple QTL *fitqtl* model, which considers QTL together to increase confidence in individual loci and looks for interactions between them.

For R/shapeQTL analyses, a multivariate Pillai trace test was used to map traits. Here, it is necessary to limit the number of variables (PCs) relative to the number of samples in order to make the estimates more robust (Maga et al., 2015; Morris et al., 2019). In these analyses, all PCs explaining >1% of the variation were included. Eight PCs (each explaining 10%, 5.5%, 2.8%, 1.8%, 1.7%, 1.4%, 1.2% and 1% of the variation, respectively) were used in the *H. melpomene* QTL analysis, whereas 9 PCs were included in the *H. erato* QTL analysis for both F2 and backcrosses (explaining 9.7%, 4.5%, 3.5%, 2.1%, 1.9%, 1.4%, 1.3%, 1.2% and 1% of the variation; Figure S3). Cumulatively, these explained only 25.4% of the overall variation in *H. melpomene* and 26.6% in *H. erato*.

We used LepBase (Challis et al., 2016) to locate the nearest gene and its Gene Ontology molecular function for markers with the highest LOD scores in significant QTL. If any previously identified *Heliconius* wing patterning loci were known to fall on a chromosome containing a QTL, we determined whether these fell within the 95% Bayesian credible intervals of these QTL.

To test for broad-scale genetic parallelism between species and to look for additive effects of multiple small effect loci, we determined the effect sizes of whole chromosomes by running a genome scan in the F2 crosses for both the univariate and multivariate traits using only maternal alleles. As there is no recombination of maternal chromosomes, maternal markers can be used to investigate chromosome-level effects. To do this, the effects of paternal markers were ignored by setting all paternal markers to be the same allele (here we used "A"). The *H. erato* and *H. melpomene* genomes are known to be highly syntenic (Kronforst et al., 2006; The Heliconius Genome Consortium, 2012; Van Belleghem et al., 2017); therefore,
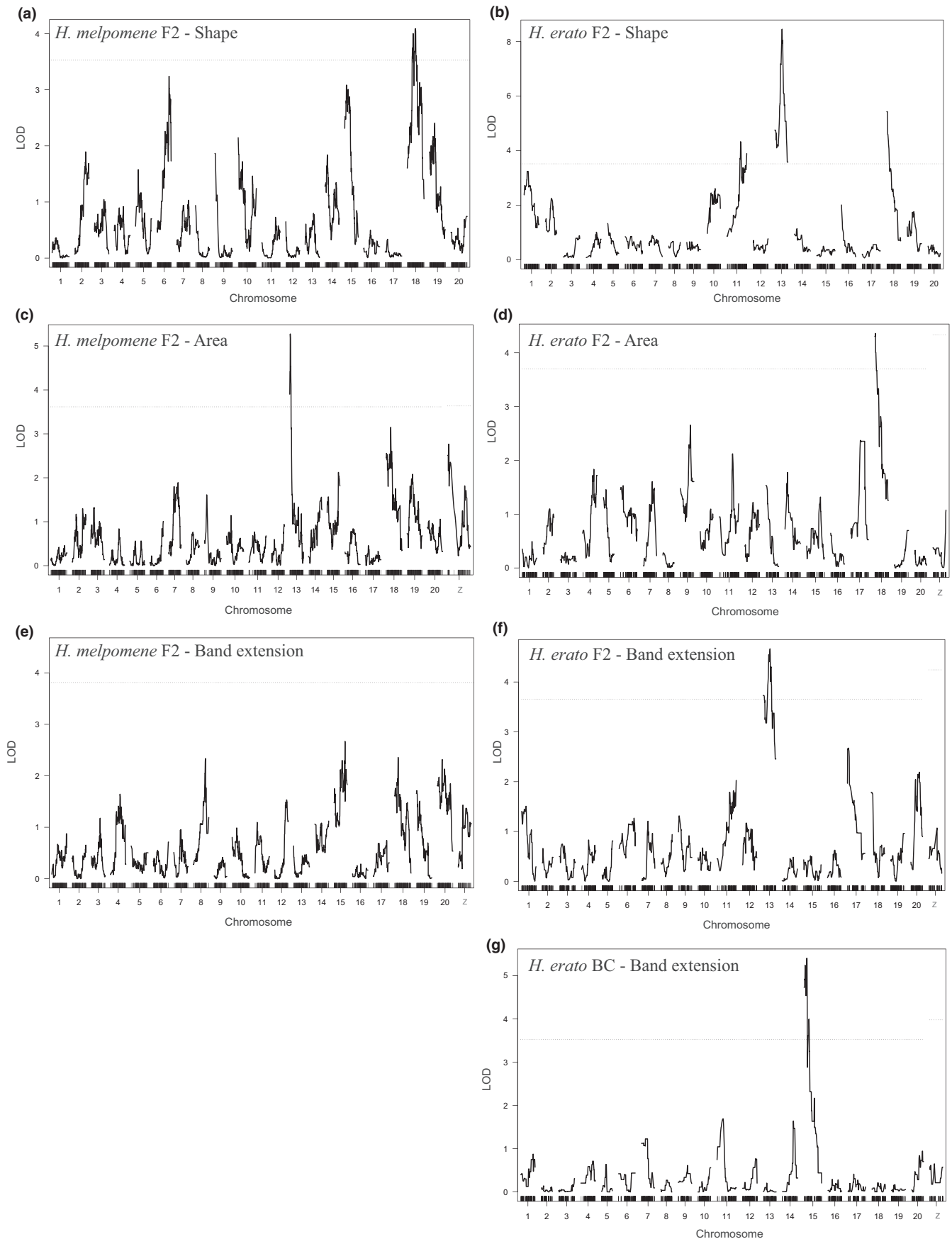
FIGURE 3 ShapeQTL scans of the F2 generation of *H. melpomene* (a) and *H. erato* (b) for the red pattern variation (captured by the PCA). Dotted lines show significance thresholds for additive LOD scores. QTL scans for relative area of the red forewing bar in F2 *H. melpomene* (c) and *H. erato* (d). QTL scans for extension of the forewing band in *H. melpomene* (e), *H. erato* F2 (f) and *H. erato* backcross (g) generations. There were no significant QTL for band extension found in *H. melpomene*

TABLE 1 All significant QTL found in the multivariate analyses for shape and univariate analyses for area and FW band extension

Trait	Marker	Chr	Position (cM)	LOD score	p-value	Lower interval	Upper interval	Toolkit gene in interval
Heliconius erato								
F2 Shape	Herato1108_6934006	11	52.2	4.32	.01	Herato1102_337589	Herato1115_96181	
	Herato1301_7929067	13	27.7	8.45	<.001	Herato1301_60743	Herato1301_10974554	
	Herato1801_1513748	18	0	5.43	<.001	Herato1801_1030457	Herato1801_2959666	Optix
BC Shape	None							
F2 Area	Herato1801_1513893	18	2	4.36	<.001	Herato1801_1030457	Herato1805_4761056	Optix
BC Area	None							
F2 FW band extension	Herato1301_7439918	13	27	4.67	.02	Herato1301_60743	Herato1301_18097294	vvl
BC FW band extension	Herato1507_3550969	15	9.95	5.4	<.001	Herato1501_26887	Herato1524_647720	Cortex
Maternal only Shape	NA	13	NA	4.12	<.001			
	NA	18	NA	5.13	<.001			
Area	NA	18	NA	2.44	<.001			
FW band extension	NA	13	NA	3.42	<.001			
Heliconius melpomene								
F2 Shape	Hmel218003o_7893652	18	38	4.09	.03	Hmel218002o_40635	Hmel218003o_14791539	Optix
Area	Hmel213001o_236599	13	10.6	5.27	.01	Hmel213001o_23517	Hmel213001o_726537	
FW band extension	None							
Maternal only Shape	NA	20	NA	4.01	.01			
Area	NA	Z	NA	2.76	.01			
FW band extension	None							

Note: Toolkit loci are noted where they occur within the 95% Bayesian intervals of the QTL. Details of toolkit loci positions within the reference genomes can be found in Table S4.
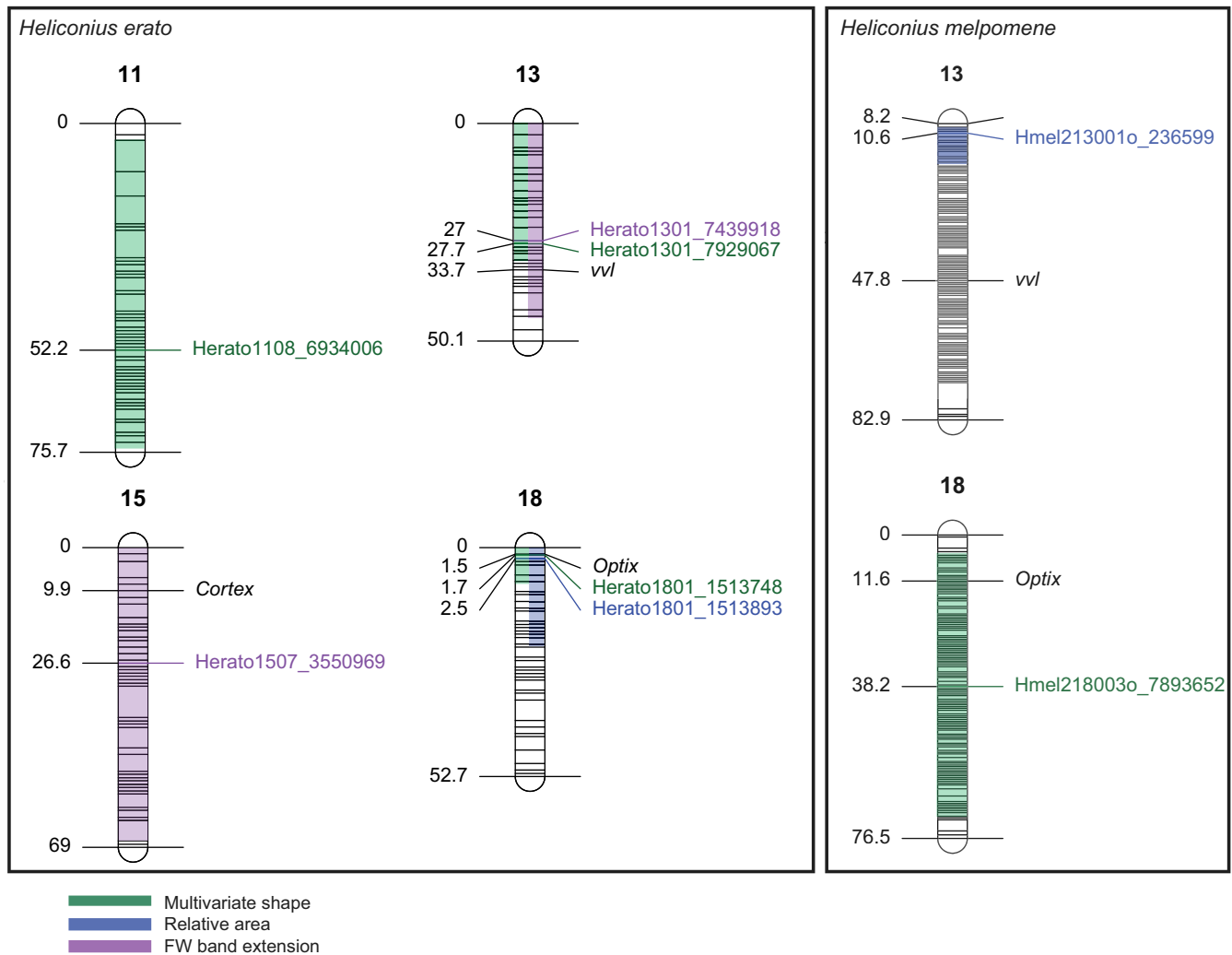
—WILEY

FIGURE 4 An overview of the locations of the QTL found in the analyses for multivariate shape (highlighted in green), relative area (blue) and FW distal band extension (purple). 95% Bayesian credible intervals are highlighted in the respective colours. Position on the linkage group (cM) is shown on the left of each chromosome, and the name of the significant markers is shown on the right. Positions of the toolkit loci (*optix*, *cortex* and *vvl*) are also shown. Figure created using LinkageMapView (Ouellette et al., 2018)

to test for parallelism we assessed whether there was a correlation between these chromosome-level effects between species, using a Spearman's rank correlation.

3 | RESULTS

3.1 | Multivariate analysis of red band shape

Heat maps were used to visualize variation in the shape of the red forewing band and compare this between *H. erato* and *H. melpomene*. Interestingly, although the heat maps for the F2 generation showed that the two species exhibited similar variation, the shape of the FW bands for *H. melpomene* and *H. erato* appears to be slightly different. *H. melpomene* showed marginally less overall variation and possessed a FW band that extended further towards the

distal edge. However, it is clear that for both species, most of the variation occurred around the border of the FW band (Figure 2a,b). The parental races were nonoverlapping in phenotypic space in the PCA. As expected for a genetically controlled trait, the F1 offspring were intermediate, with F2 offspring having a wider distribution of phenotypic values that overlap with those of the parental races, and backcross offspring being skewed towards the backcross parent (Figure 2c,d).

To find genomic regions controlling the variation captured by the PCA, QTL scans were conducted for the F2 generations of both species and for the *H. erato* BC family. No LOD scores were above the significance threshold for the BC generation. However, in the *H. erato* F2 generation, three QTL were found on chromosomes 11, 13 and 18. These explained 3.4%, 4.6% and 5.9% of the variation in FW red colour pattern, respectively. For *H. melpomene*, a single significant QTL was found, also on chromosome 18. This explained 4.3% of the variation
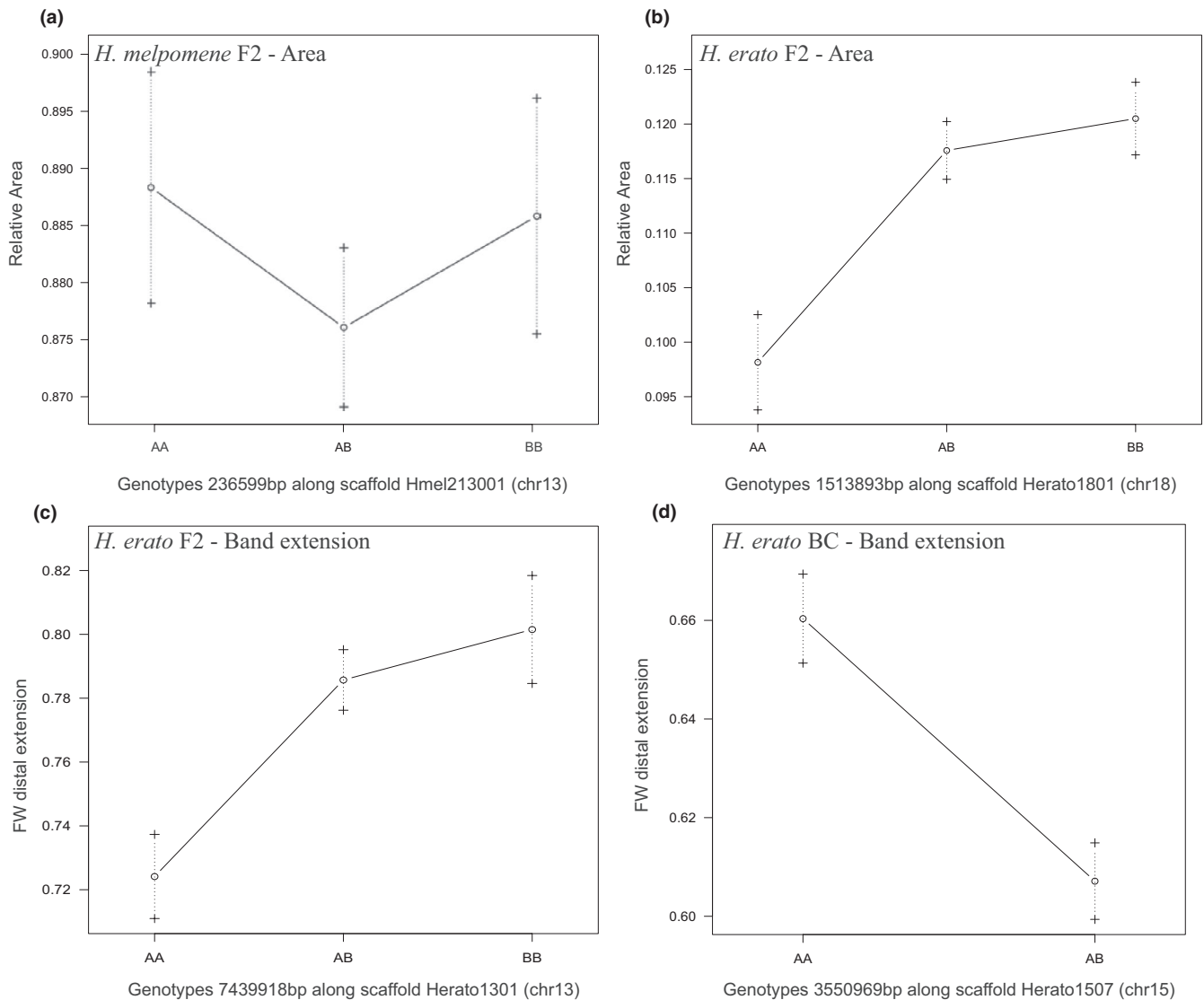
(a) *H. melpomene* F2 - Area

(b) *H. erato* F2 - Area

(c) *H. erato* F2 - Band extension

(d) *H. erato* BC - Band extension

FIGURE 5 Effect plots showing the FW band area phenotype means for each group in the F2 generation of *H. melpomene* (a) and *H. erato* (b), defined by the genotypes at the respective markers. Effect plots showing the phenotype means for FW band extension in the *H. erato* F2 (c) and BC generations (d). The 'A' alleles are from the iridescent race (*H. m. cythera* and *H. e. cyrbia*) and the 'B' alleles from the noniridescent race (*H. m. rosina*, *H. e. demophoon*)

(Figure 3a,b and Table 1). Chromosomes 13 and 18 harbour the known "toolkit" loci *Ro* (*vvl*) and *optix*, respectively. In both species, the 95% Bayesian credible intervals on chromosome 18 overlapped with the gene *optix* (Figure 4), although the interval was large in *H. melpomene*, spanning almost the entire chromosome. In the *H. erato* map, the marker with the highest LOD score was only 1.5 cM from the position of *optix*. The 95% Bayesian credible interval of the QTL on *H. erato* chromosome 13, however, did not contain the gene *vvl*.

3.2 | Univariate analysis of relative area of the FW band

We also performed QTL mapping of the univariate trait, relative area of the red FW band, in both species. As with the multivariate trait

analysis, no LOD scores were found above the significance threshold for the backcross generation. However, for the F2 generations of both *H. melpomene* and *H. erato*, single significant QTL were found (Figure 3c,d). In *H. melpomene*, this was on chromosome 13 (LOD = 5.27, p = .01) and explained 17.4% of the variation, and in *H. erato*, the QTL was on chromosome 18 (LOD = 4.36, p < .001) and explained 18.9% of the variation. *Optix* was within the 95% Bayesian credible intervals for the *H. erato* chromosome 18 QTL, and thus could be a candidate locus here (Figure 4, Table 1). The gene *vvl* was not within the 95% Bayesian credible interval for the *H. melpomene* chromosome 13 QTL.

Effect plots show that in *H. erato*, heterozygotes for the chromosome 18 marker were on average closer in phenotype to homozygotes for the *demophoon* (the Panama subspecies with large red bar) allele than homozygotes for the *cyrbia* allele, suggesting slight

dominance of *demophoon*, consistent with the general pattern whereby the presence of red pattern elements controlled by *optix* tends to be dominant. In contrast, in *H. melpomene*, heterozygotes for the chromosome 13 marker expressed slightly smaller FW bands than either homozygote, sometimes referred to as "underdominance" (Figure 5a,b).

3.3 | Variation in the distal extension of the red FW band

To further investigate how the collection of phenotypic data altered the loci identified, we phenotyped and mapped individuals for the distal extension of the red FW band using more "traditional" linear measurements (rather than pixel-based pattern extraction). No significant QTL were found for *H. melpomene* (Figure 3e). However, in *H. erato*, the F2 generation had a single QTL on chromosome 13 (LOD = 4.67, p = .02), whereas in the BC generation, a single significant QTL was found on chromosome 15 (LOD = 5.40, p < .001) (Figure 3f,g). The QTL on chromosomes 13 and 15 included *vvl* and *cortex*, respectively, within their 95% credible intervals, although the intervals are large (Figure 4, Table 1). The loci explained 19.5% and 23.4% of the variation in the extension of the FW band in the F2 and BC generations, respectively.

In the F2 generation of *H. erato*, the *demophoon* allele for the QTL on chromosome 13 produced a more extended bar and showed slight dominance over the *cyrbia* allele. For the backcross generation, only two genotypes are possible (homozygote *cyrbia* or heterozygote). Surprisingly, individuals with a *cyrbia* genotype at the chromosome 15 locus had longer measures for the distal extension than heterozygotes (Figure 5c,d).

3.4 | Chromosome-level analysis to investigate the level of genetic parallelism

Small effect loci are likely to be missed in QTL analyses with small sample sizes due to lack of power. However, using a chromosome-level analysis, we can look at the combined effects of multiple small effect loci. For example, if there are many small effect loci on a single linkage group, these may not be detected in the full genome scan, but the additive LOD scores could reach significance when comparing effect sizes of whole chromosomes. This can then be used to compare genetic architecture between species. This comparison of maternal alleles provides further evidence for differences in genetics of this trait between species, as there are no parallel significant chromosomes. For *H. erato*, the results are very similar to those found with all markers, although only chromosomes 13 and 18 are detected as significant, with both affecting the multivariate trait, and 18 and 13 affecting the area and linear measurements, respectively (Table 1, Figure S4).

For *H. melpomene*, chromosome 20 was found to significantly affect the multivariate trait (LOD = 4.01, p = .01), which was not seen when all markers were used, suggesting there may be multiple small effect loci located on this chromosome. LOD scores for both the area and distal extension analyses were very low in *H. melpomene*, but the Z chromosome had the highest LOD score for both, with a significant effect on area (Table 1).

To test for parallelism in the combined effect of all markers on each chromosome, we compared the variance explained by each chromosome in *H. erato* and *H. melpomene* and found no correlation between the species in either relative area (r_{19} = 0.16, p = .48) or FW band extension (r_{19} = 0.09, p = .71; Figure S5). The maternal chromosomes explain little of the overall variation in area, around 15% and 32% in *H. melpomene* and *H. erato*, respectively. For FW band extension, 28% of the variation is explained in both species. However, this is not unexpected because the most that these maternal genotypes can explain is 50%, with the rest of the genetic variance coming from the paternal markers.

4 | DISCUSSION

Our analysis shows that complex variation in the size and shape of red pattern elements, in both *H. melpomene* and *H. erato*, is controlled by a small number of medium to large effect loci. The small amount of phenotypic variation explained by these loci suggests there are likely more loci of minor effect involved. These findings are broadly consistent with the theoretical prediction that an adaptive walk follows a "two-step" process, where single large effect loci evolve initially (during large trait shifts), but smaller modifier loci evolve later to refine the subtle variation (Nicholson, 1927; Orr, 1998; Sheppard et al., 1985). To some extent, our results support other recent studies asserting that multivariate QTL scans are better able to capture the full magnitude or direction of shape changes, compared with univariate measurements (Maga et al., 2015; Pallares et al., 2016; Rossato et al., 2018). Nevertheless, in both species we only detect one additional QTL that was not detected by either of the univariate measurements. In addition, in both species we find QTL in the univariate analysis that were not detected in the multivariate analysis, for example the QTL on chromosome 15 in *H. erato* was found in a univariate but not multivariate scan. These two types of analysis could be capturing slightly different aspects of the phenotype, in particular variation explained by the PCs not included in the shape analysis.

A major question asked by this study was whether repeated evolution between converging species is reflected by the same or different genetic changes (Nadeau et al., 2014; Ng et al., 2008; Parchem et al., 2007). Although the known major effect locus *optix* was reused in both species, we found less evidence for genetic parallelism between small effect loci. The transcription factor *optix* already has a well-defined role in the colour fate of scale cells acting as a switch-like regulator between orange/red (ommochrome) and black/grey (melanin) patterns (Baxter et al., 2008; Nadeau et al., 2014; Reed et al., 2011). Our results are consistent with previous QTL studies and recent gene editing experiments, which have found that genetic

variation around the *optix* gene can also have subtle effects on the size and shape of red pattern elements (Lewis et al., 2019).

Along with *optix*, other loci control variation in size and shape of these red elements (Nadeau, 2016). The most prominent of these is the *WntA* gene on chromosome 10, which has been shown to control the placement of melanic scales in both *H. melpomene* and *H. erato* (Concha et al., 2019; Jiggins, 2017; Martin et al., 2012; Naisbit et al., 2003). As we specifically investigated shape differences in red FW pattern elements, it is surprising that we did not find any QTL, which might contain *WntA*. This result indicates that the shape of red pattern elements studied in the crosses here may follow a divergent process to what has been studied in other crosses previously, and that alleles other than those contained within *WntA* are having an effect here. Alternatively, our QTL analysis may have been unable to detect effects of *WntA* with the sample sizes used here, if they had a small effect (Beavis, 1998). The linkage maps for both species had a marker less than 170kbp from the position of *WntA*, so it is likely that any medium to large effect alleles at this locus would have been detected.

In contrast, we do find QTL on chromosome 13 containing the *vvl* gene. This locus is less well studied but has previously been identified as controlling forewing band shape variation in both *H. erato* (Nadeau et al., 2014; Sheppard et al., 1985; Van Belleghem et al., 2017) and *H. melpomene* (Baxter et al., 2009; Morris et al., 2019). Our finding of a QTL for distal extension of the forewing band that overlaps with the gene *cortex* in *H. erato* is more surprising. Often, *cortex* is described as having control over yellow/white (rather than red) wing pattern elements in both species (Joron et al., 2006; Nadeau, 2016). However, some studies have begun to acknowledge the potential alternative effects of this locus. Nadeau (2016) suggested that the effect of *cortex* on colour might vary with the developmental stage that it is upregulated in, whereas others have found evidence for an epistatic interaction between *cortex* and *optix* in *H. melpomene* (Martin et al., 2014; Salazar, 2012). Thus, it is possible that *cortex* is controlling red band shape through an epistatic relationship with *optix*, which may explain why it is detected in the backcross but not the intercross F2.

Two novel patterning loci were identified on chromosomes 11 and 13. These QTL likely represent some of the small effect loci that form the latter half of the hypothesized "two-step" model (Orr, 1998). No previous studies have identified a locus controlling forewing red pattern variation on chromosome 11 in either species, and we appear to identify a locus on chromosome 13 that does not overlap with *vvl*.

With the sample sizes analysed, we lack the power to detect loci of small effect and our multivariate analysis explained about 25% of the total variation in shape. Therefore, it is completely possible that there are parallels in minor effect loci between species that we simply fail to detect. Nevertheless, further support for a lack of genetic parallelism comes from the analysis of only maternal alleles, where minor effects will be summed across the whole chromosome. We do not see evidence of the same chromosomes containing genes for

forewing band patterning across species. However, to be detected as significant, the cumulative effect of the loci across the chromosome would need to be somewhat greater than the effect of a single locus found in the scans using the full data, as variation coming from the paternal chromosomes will act as additional noise in this analysis. Although the scans for *H. erato* showed the same chromosomes to be significant as the full analysis (13 and 18), scans of *H. melpomene* revealed chromosomes 20 and Z as significant. These were not seen in the full analysis, suggesting there may be multiple small effect loci on these chromosomes. There is previous evidence for a locus controlling forewing band shape on chromosome 20 in *H. melpomene* (Nadeau et al., 2014), which could be a possible candidate. The Z result could reflect sexual dimorphism rather than sex linkage. Most of these offspring are from one cross direction, so sex and maternal Z genotype are highly confounded in this analysis: only males will inherit a maternal Z chromosome (females inherit a W, which we lack markers for), and this will almost exclusively by from the *cythera* grandparent (with the exception of seven individuals that had a *rosina* maternal grandfather).

When phenotypic convergence is reflected by convergent genetic mechanisms, it supports the idea that genetic evolution is fairly constrained, and therefore that adaptive evolution may be predictable (Losos, 2011; Stern & Orgogozo, 2008). Comparative mapping studies in *Heliconius* find evidence for homologous wing patterning loci, thus leading to a general perception that genetic evolution is surprisingly repeatable (Martin et al., 2014; Papa et al., 2008). However, despite finding genetic parallels with *optix* in this study, other QTL identified do not show similarities. In addition, the phenotypic effect of *optix* appears to differ between species, with an effect on band area in *H. erato* but only on band shape in *H. melpomene*. This suggests that evolution at the genetic level in *Heliconius* is not as predictable as first thought, thus indicating that perhaps large phenotypic changes, relating to the initial steps of the hypothesized "two-step" model, are much more constrained, and therefore repeatable, than the latter half of the model (relating to subtler trait shifts).

A question that then remains is, what makes certain loci more likely to evolve in parallel over others? It is possible that finding genetic "hot spots" is a mere reflectance of biases in the research; focusing on known candidate genes is considerably easier than identifying novel ones (Conte et al., 2012). Additionally, identifying QTL of large effect is easier than identifying those of small effect (Rockman, 2011). One reason that certain loci are highly re-used in adaptation, whereas others are not, could be their genetic architecture. *Optix* has been shown to have a complex modular architecture, consisting of multiple cis-regulatory modules (Van Belleghem et al., 2017; Reed et al., 2011; Wallbank et al., 2016). Pleiotropy, where a gene affects multiple different traits, is often assumed to be purged in evolution as it rarely results in solely advantageous changes. However, genes that are able to integrate multiple upstream regulatory elements and, in turn, alter specific phenotypes without causing any knock-on deleterious effects will be favoured in adaptive evolution (Stern & Orgogozo, 2008; Gompel and Prud'homme

2009). Thus, it could be hypothesized that these loci have become "hot spots" for adaptive change across the *Heliconius* genus due to their ability to guide large effect mutations, without deleterious effects on other traits (Jiggins, 2017; Pavličev & Cheverud, 2015; Reed et al., 2011).

5 | CONCLUSION

Previous studies have often focused on major effect loci that affect discrete pattern changes in *Heliconius*. In contrast, this study has demonstrated that, with multivariate trait analysis, QTL mapping can be used to identify a greater number of smaller effect loci in a single analysis, in turn questioning the role of a simple genetic "toolkit" in *Heliconius*. Combining this study with previous findings builds a picture of a genetic architecture that is consistent with the theoretical "two-step" model of evolution. However, finding that genetic parallels are not as widespread as first expected suggests that the individual path each species takes along this adaptive walk is likely less predictable than previously thought.

CONFLICT OF INTEREST
The authors declare we have no conflict of interest.

AUTHOR CONTRIBUTIONS
HEB and MNB performed the analyses. PR and MNB constructed the linkage maps. PAS, CM, MNB and NJN performed the crosses. NJN devised and co-ordinated the study. HEB and MNB wrote the manuscript. All authors read and commented on the manuscript.

PEER REVIEW
The peer review history for this article is available at https://publons.com/publon/10.1111/jeb.13704.

DATA AVAILABILITY STATEMENT
Sequence data have been deposited in the European Nucleotide Archive under project number PRJEB38330. Photographs of all samples can be found at https://doi.org/10.5281/zenodo.3799188. Linkage maps and all phenotypic measurements used were uploaded to Dryad https://doi.org/10.5061/dryad.5dv41ns4g.

ORCID
Melanie N. Brien 🔟 https://orcid.org/0000-0002-3089-4776
Nicola J. Nadeau 🔟 https://orcid.org/0000-0002-9319-921X

REFERENCES

Arendt, J., & Reznick, D. (2008). Convergence and parallelism reconsidered: What have we learned about the genetics of adaptation? *Trends in Ecology and Evolution*, 23, 26–32.

Baxter, S. W., Davey, J. W., Johnston, J. S., Shelton, A. M., Heckel, D. G., Jiggins, C. D., & Blaxter, M. L. (2011). Linkage mapping and comparative genomics using next-generation rad sequencing of a nonmodel organism. *PLoS One*, 6, e19315. https://doi.org/10.1371/journal.pone.0019315

Baxter, S., Johnston, S., & Jiggins, C. (2009). Butterfly speciation and the distribution of gene effect sizes fixed during adaptation. *Heredity*, 102, 57–65. https://doi.org/10.1038/hdy.2008.109

Baxter, S. W., Papa, R., Chamberlain, N., Humphray, S. J., Joron, M., Morrison, C., Ffrench-Constant, R. H., McMillan, W. O., & Jiggins, C. D. (2008). Convergent evolution in the genetic basis of Müllerian Mimicry in *Heliconius* Butterflies. *Genetics*, 180, 1567–1577. https://doi.org/10.1534/genetics.107.082982

Beavis, W. (1998). QTL analyses: Power, precision, and accuracy. In A. H. Paterson (Ed.), *Molecular dissection of complex traits* (pp. 145–162). CRC Press.

Benson, W. W. (1972). Natural selection for Müllerian Mimicry in *Heliconius erato* in Costa Rica. *Science*, 176, 936–939.

Brien, M. N., Enciso-Romero, J., Parnell, A. J., Morochz, C., Chalá, D., Salazar, P. A., Bainbridge, H. E., Zinn, T., Curran, E. V., & Nadeau, N. J. (2018). Phenotypic variation in *Heliconius erato* crosses shows that iridescent structural colour is sex-linked and controlled by multiple genes. *Interface Focus*, 9, 20180047.

Broman, K., & Sen, S. (2009). *A guide to QTL mapping with R/qtl*. Springer.

Broman, K. W., Sen, Ś., Owens, S. E., Manichaikul, A., Southard-Smith, E. M., & Churchill, G. A. (2006). The X chromosome in quantitative trait locus mapping. *Genetics*, 174, 2151–2158. https://doi.org/10.1534/genetics.106.061176

Challis, R. J., Kumar, S., Dasmahapatra, K. K., Jiggins, C. D., & Blaxter, M. (2016). Lepbase: The Lepidopteran genome database. *bioRxiv*, 056994.

Churchill, G. A., & Doerge, R. W. (1994). Empirical threshold values for quantitative trait mapping. *Genetics*, 138, 963–971.

Colosimo, P. F., Hosemann, K. E., Balabhadra, S., Villarreal, G., Dickson, M., Grimwood, J., Schmutz, J., Myers, R. M., Schluter, D., & Kingsley, D. M. (2005). Widespread parallel evolution in sticklebacks by repeated fixation of ectodysplasin alleles. *Science*, 30, 1928–1933. https://doi.org/10.1126/science.1107239

Concha, C., Wallbank, R. W. R., Hanly, J. J., Fenner, J., Livraghi, L., Santiago Rivera, E., … McMillan, W. O. (2019). Interplay between developmental flexibility and determinism in the evolution of mimetic heliconius wing patterns. *Current Biology*, 29(23), 3996–4009. https://doi.org/10.1016/j.cub.2019.10.010

Conte, G. L., Arnegard, M. E., Peichel, C. L., & Schluter, D. (2012). The probability of genetic parallelism and convergence in natural populations. *Proceedings of the Royal Society B: Biological Sciences*, 279, 5039–5047. https://doi.org/10.1098/rspb.2012.2146

Davey, J. W., Barker, S. L., Rastas, P. M., Pinharanda, A., Martin, S. H., Durbin, R., McMillan, W. O., Merrill, R. M., & Jiggins, C. D. (2017). No evidence for maintenance of a sympatric *Heliconius* species barrier by chromosomal inversions. *Evolution Letters*, 1, 138–154.

de Celis, J. F., Llimargas, M., & Casanova, J. (1995). *ventral veinless*, the gene encoding the Cf1a transcription factor, links positional information and cell differentiation during embryonic and imaginal development in *Drosophila melanogaster*. *Development*, 121, 3405–3416.

Fisher, R. A. (1930). *The genetical theory of natural selection*. Oxford University Press.

Gompel, N., & Prud'homme, B. (2009). The causes of repeated genetic evolution. *Developmental Biology*, 332, 36–47. https://doi.org/10.1016/j.ydbio.2009.04.040

Hemingson, C. R., Cowman, P. F., Hodge, J. R., & Bellwood, D. R. (2019). Colour pattern divergence in reef fish species is rapid and driven by both range overlap and symmetry. *Ecology Letters*, *22*, 190–199. https://doi.org/10.1111/ele.13180

Hines, H. M., Counterman, B. A., Papa, R., Albuquerque de Moura, P., Cardoso, M. Z., Linares, M., Mallet, J., Reed, R. D., Jiggins, C. D., Kronforst, M. R., & McMillan, W. O. (2011). Wing patterning gene redefines the mimetic history of *Heliconius* butterflies. *Proceedings of the National Academy of Sciences of the United States of America*, *108*, 19666–19671. https://doi.org/10.1073/pnas.1110096108

Hoekstra, H. E., & Nachman, M. W. (2003). Different genes underlie adaptive melanism in different populations of rock pocket mice. *Molecular Ecology*, *12*, 1185–1194. https://doi.org/10.1046/j.1365-294X.2003.01788.x

Huber, B., Whibley, A., Poul, Y. L., Navarro, N., Martin, A., Baxter, S., Shah, A., Gilles, B., Wirth, T., McMillan, W. O., & Joron, M. (2015). Conservatism and novelty in the genetic architecture of adaptation in *Heliconius* butterflies. *Heredity*, *114*, 515–524. https://doi.org/10.1038/hdy.2015.22

Jiggins, C. D. (2017). *The ecology & evolution of Heliconius butterflies*. Oxford University Press.

Jones, R. T., Salazar, P. A., Ffrench-Constant, R. H., Jiggins, C. D., & Joron, M. (2012). Evolution of a mimicry supergene from a multilocus architecture. *Proceedings of the Royal Society B: Biological Sciences*, *279*, 316–325. https://doi.org/10.1098/rspb.2011.0882

Joron, M., Papa, R., Beltrán, M., Chamberlain, N., Mavárez, J., Baxter, S., Abanto, M., Bermingham, E., Humphray, S. J., Rogers, J., Beasley, H., Barlow, K., H. ffrench-Constant, R., Mallet, J., McMillan, W. O., & Jiggins, C. D. (2006). A conserved supergene locus controls colour pattern diversity in *Heliconius* Butterflies. *PLoS Biology*, *4*, 1831–1840. https://doi.org/10.1371/journal.pbio.0040303

Klein, A. L., & de Araújo, A. M. (2013). Sexual size dimorphism in the color pattern elements of two mimetic *Heliconius* Butterflies. *Neotropical Entomology*, *42*, 600–606. https://doi.org/10.1007/s13744-013-0157-x

Kronforst, M. R., Kapan, D. D., & Gilbert, L. E. (2006). Parallel genetic architecture of parallel adaptive radiations in mimetic *Heliconius* butterflies. *Genetics*, *174*, 535–539. https://doi.org/10.1534/genetics.106.059527

Langmead, B., & Salzberg, S. L. (2012). Fast gapped-read alignment with Bowtie 2. *Nature Methods*, *9*, 357. https://doi.org/10.1038/nmeth.1923

Lee, D. E., Cavener, D. R., & Bond, M. L. (2018). Seeing spots: Quantifying mother-offspring similarity and assessing fitness consequences of coat pattern traits in a wild population of giraffes (*Giraffa camelopardalis*). *PeerJ*, *6*, e5690.

Lewis, J. J., Geltman, R. C., Pollak, P. C., Rondem, K. E., van Belleghem, S. M., Hubisz, M. J., Munn, P. R., Zhang, L., Benson, C., Mazo-Vargas, A., Danko, C. G., Counterman, B. A., Papa, R., & Reed, R. D. (2019). Parallel evolution of ancient, pleiotropic enhancers underlies butterfly wing pattern mimicry. *Proceedings of the National Academy of Sciences of the United States of America*, *116*, 24174–24183. https://doi.org/10.1073/pnas.1907068116

Li, H. (2011). A statistical framework for SNP calling, mutation discovery. *Bioinformatics*, *27*, 2987–2993.

Losos, J. B. (2011). Convergence, adaptation, and constraint. *Evolution*, *65*, 1827–1840. https://doi.org/10.1111/j.1558-5646.2011.01289.x

Maga, A. M., Navarro, N., Cunningham, M. L., & Cox, T. C. (2015). Quantitative trait loci affecting the 3D skull shape and size in mouse and prioritization of candidate genes in-silico. *Frontiers in Physiology*, *6*, 92. https://doi.org/10.3389/fphys.2015.00092

Martin, A., McCulloch, K. J., Patel, N. H., Briscoe, A. D., Gilbert, L. E., & Reed, R. D. (2014). Multiple recent co-options of *Optix* associated with novel traits in adaptive butterfly wing radiations. *EvoDevo*, *5*, 7. https://doi.org/10.1186/2041-9139-5-7

Martin, A., Papa, R., Nadeau, N. J., Hill, R. I., Counterman, B. A., Halder, G., Jiggins, C. D., Kronforst, M. R., Long, A. D., McMillan, W. O., & Reed, R. D. (2012). Diversification of complex butterfly wing patterns by repeated regulatory evolution of a *Wnt* ligand. *Proceedings of the National Academy of Sciences of the United States of America*, *109*, 12632–12637. https://doi.org/10.1073/pnas.1204800109

Morris, J., Navarro, N., Rastas, P., Rawlins, L. D., Sammy, J., Mallet, J., & Dasmahapatra, K. K. (2019). The genetic architecture of adaptation: Convergence and pleiotropy in *Heliconius* wing pattern evolution. *Heredity*, *123*, 138–152. https://doi.org/10.1038/s41437-018-0180-0

Nadeau, N. J. (2016). Genes controlling mimetic colour pattern variation in butterflies. *Current Opinion in Insect Science*, *17*, 24–31. https://doi.org/10.1016/j.cois.2016.05.013

Nadeau, N. J., & Jiggins, C. D. (2010). A golden age for evolutionary genetics? Genomic studies of adaptation in natural populations. *Trends in Genetics*, *26*, 484–492. https://doi.org/10.1016/j.tig.2010.08.004

Nadeau, N. J., Ruiz, M., Salazar, P., Counterman, B., Medina, J. A., Ortiz-Zuazaga, H., Morrison, A., McMillan, W. O., Jiggins, C. D., & Papa, R. (2014). Population genomics of parallel hybrid zones in the mimetic butterflies, *H. melpomene* and *H. erato*. *Genome Research*, *24*, 1316–1333.

Naisbit, R. E., Jiggins, C. D., & Mallet, J. (2003). Mimicry: Developmental genes that contribute to speciation. *Evolution and Development*, *5*, 269–280. https://doi.org/10.1046/j.1525-142X.2003.03034.x

Navarro, N. (2015). *R/shapeQTL: Shape QTL mapping experiment with R*. Retrieved from github.com/nnavarro/shapeQTL

Ng, C. S., Hamilton, A. M., Frank, A., Barmina, O., & Kopp, A. (2008). Genetic basis of sex-specific color pattern variation in *Drosophila malerkotliana*. *Genetics*, *180*, 421–429.

Nicholson, A. (1927). *A new theory of insects*. Royal Zoological Society of New South Wales.

Orr, H. A. (1998). The population genetics of adaptation: The distribution of factors fixed during adaptive evolution. *Evolution*, *52*, 935–949. https://doi.org/10.1111/j.1558-5646.1998.tb01823.x

Ouellette, L., Reid, R., Blanchard, S., & Brouwer, C. (2018). LinkageMapView - rendering high-resolution linkage and QTL maps. *Bioinformatics*, *34*, 306–307. https://doi.org/10.1093/bioinformatics/btx576

Pallares, L. F., Turner, L. M., & Tautz, D. (2016). Craniofacial shape transition across the house mouse hybrid zone: Implications for the genetic architecture and evolution of between-species differences. *Development Genes and Evolution.*, *226*, 173–186. https://doi.org/10.1007/s00427-016-0550-7

Papa, R., Kapan, D. D., Counterman, B. A., Maldonado, K., Lindstrom, D. P., Reed, R. D., Nijhout, H. F., Hrbek, T., & McMillan, W. O. (2013). Multi-allelic major effect genes interact with minor effect QTLs to control adaptive color pattern variation in *Heliconius erato*. *PLoS One*, *8*, e57033. https://doi.org/10.1371/journal.pone.0057033

Papa, R., Martin, A., & Reed, R. D. (2008). Genomic hotspots of adaptation in butterfly wing pattern evolution. *Current Opinion in Genetics and Development*, *18*, 559–564. https://doi.org/10.1016/j.gde.2008.11.007

Parchem, R. J., Perry, M. W., & Patel, N. H. (2007). Patterns on the insect wing. *Current Opinion in Genetics and Development*, *17*, 300–308. https://doi.org/10.1016/j.gde.2007.05.006

Pavličev, M., & Cheverud, J. M. (2015). Constraints evolve: Context dependency of gene effects allows evolution of pleiotropy. *Annual Review of Ecology, Evolution, and Systematics*, *46*, 413–434. https://doi.org/10.1146/annurev-ecolsys-120213-091721

R Core Team (2018). *R: A language and environment for statistical computing*. R Foundation for Statistical Computing.

Rastas, P. (2017). Lep-MAP3: Robust linkage mapping even for low-coverage whole genome sequencing data. *Bioinformatics*, *33*, 3726–3732. https://doi.org/10.1093/bioinformatics/btx494

Reed, R. D., Papa, R., Martin, A., Hines, H. M., Counterman, B. A., Pardo-Diaz, C., Jiggins, C. D., Chamberlain, N. L., Kronforst, M. R., Chen, R., Halder, G., Nijhout, H. F., & McMillan, W. O. (2011). *optix* drives the repeated convergent evolution of butterfly wing pattern mimicry. *Science*, *333*, 1137–1141. https://doi.org/10.1126/science.1208227

Rockman, M. V. (2011). The QTN program and the alleles that matter for evolution: All that's gold does not glitter. *Evolution*, *66*, 1–17.

Roelants, K., Fry, B. G., Norman, J. A., Clynen, E., Schoofs, L., & Bossuyt, F. (2010). Identical skin toxins by convergent molecular adaptation in frogs. *Current Biology*, *20*, 125–130. https://doi.org/10.1016/j.cub.2009.11.015

Rossato, D. O., Boligon, D., Fornel, R., Kronforst, M. R., Gonçalves, G. L., & Moreira, G. R. P. (2018). Subtle variation in size and shape of the whole forewing and the red band among co-mimics revealed by geometric morphometric analysis in *Heliconius* butterflies. *Ecology and Evolution*, *8*, 3280–3295.

Salazar, P. A. (2012). *Hybridization and the genetics of wing colour-pattern diversity in Heliconius butterflies*. Thesis: University of Cambridge.

Schindelin, J., Arganda-Carreras, I., Frise, E., Kaynig, V., Longair, M., Pietzsch, T., Preibisch, S., Rueden, C., Saalfeld, S., Schmid, B., Tinevez, J.-Y., White, D. J., Hartenstein, V., Eliceiri, K., Tomancak, P., & Cardona, A. (2012). Fiji: An open-source platform for biological-image analysis. *Nature Methods*, *9*, 676–682. https://doi.org/10.1038/nmeth.2019

Schmitz, S., Cherny, S. S., & Fulker, D. W. (1998). Increase in power through multivariate analyses. *Behavioural Genetics*, *28*, 357–363.

Shapiro, M. D., Marks, M. E., Peichel, C. L., Blackman, B. K., Nereng, K. S., Jónsson, B., Schluter, D., & Kingsley, D. M. (2004). Genetic and developmental basis of evolutionary pelvic reduction in threespine sticklebacks. *Nature*, *428*, 717–723. https://doi.org/10.1038/nature02415

Sheppard, P. M., Turner, J. R. G., Brown, K. S., Benson, W. W., & Singer, M. C. (1985). Genetics and the Evolution of Mullerian Mimicry in *Heliconius* Butterflies. *Philosophical Transactions of the Royal Society B: Biological Sciences*, *308*, 433–610.

Stern, D. L. (2013). The genetic causes of convergent evolution. *Nature Reviews Genetics*, *14*, 751–764. https://doi.org/10.1038/nrg3483

Stern, D. L., & Orgogozo, V. (2008). The loci of evolution: How predictable is genetic evolution? *Evolution*, *62*, 2155–2177. https://doi.org/10.1111/j.1558-5646.2008.00450.x

Suomalainen, E., Cook, L., & Turner, J. (1973). Achiasmatic oogenesis in the Heliconiine butterflies. *Hereditas*, *74*, 302–304. https://doi.org/10.1111/j.1601-5223.1973.tb01134.x

The Heliconius Genome Consortium (2012). Butterfly genome reveals promiscuous exchange of mimicry adaptations among species. *Nature*, *487*, 94–98.

Van Belleghem, S. M., Papa, R., Ortiz-Zuazaga, H., Hendrickx, F., Jiggins, C. D., Owen McMillan, W., & Counterman, B. A. (2018). patternize: An R package for quantifying colour pattern variation. *Methods in Ecology and Evolution*, *9*, 390–398. https://doi.org/10.1111/2041-210X.12853

Van Belleghem, S. M., Rastas, P., Papanicolaou, A., Martin, S. H., Arias, C. F., Supple, M. A., Hanly, J. J., Mallet, J., Lewis, J. J., Hines, H. M., Ruiz, M., Salazar, C., Linares, M., Moreira, G. R. P., Jiggins, C. D., Counterman, B. A., McMillan, W. O., & Papa, R. (2017). Complex modular architecture around a simple toolkit of wing pattern genes. *Nature Ecology and Evolution*, *1*, 1–12. https://doi.org/10.1038/s41559-016-0052

Wallbank, R. W. R., Baxter, S. W., Pardo-Diaz, C., Hanly, J. J., Martin, S. H., Mallet, J., Dasmahapatra, K. K., Salazar, C., Joron, M., Nadeau, N., McMillan, W. O., & Jiggins, C. D. (2016). Evolutionary novelty in a butterfly wing pattern through enhancer shuffling. *PLoS Biology*, *14*, 1–16. https://doi.org/10.1371/journal.pbio.1002353

Westerman, E. L., VanKuren, N. W., Massardo, D., Tenger-Trolander, A., Zhang, W., Hill, R. I., … Kronforst, M. R. (2018). Aristaless controls butterfly wing color variation used in mimicry and mate choice. *Current Biology*, *28*(21), 3469–3474. http://dx.doi.org/10.1016/j.cub.2018.08.051

Wood, T. E., Burke, J. M., & Rieseberg, L. H. (2005). Parallel genotypic adaptation: When evolution repeats itself. *Genetica*, *123*, 157–170. https://doi.org/10.1007/s10709-003-2738-9

SUPPORTING INFORMATION

Additional supporting information may be found online in the Supporting Information section.